Temporal Analysis of Sucrose-induced Phosphorylation Changes in Plasma Membrane Proteins of *Arabidopsis**[S]

Totte Niittylä‡§, Anja T. Fuglsang§¶, Michael G. Palmgren¶, Wolf B. Frommer‡, and Waltraud X. Schulze‖**

Sucrose is the main product of photosynthesis and the most common transport form of carbon in plants. In addition, sucrose is a compound that serves as a signal affecting metabolic flux and development. Here we provide first results of externally induced phosphorylation changes of plasma membrane proteins in *Arabidopsis*. In an unbiased approach, seedlings were grown in liquid medium with sucrose and then depleted of carbon before sucrose was resupplied. Plasma membranes were purified, and phosphopeptides were enriched and subsequently analyzed quantitatively by mass spectrometry. In total, 67 phosphopeptides were identified, most of which were quantified over five time points of sucrose resupply. Among the identified phosphorylation sites, the well described phosphorylation site at the C terminus of plasma membrane H^+-ATPases showed a relative increase in phosphorylation level in response to sucrose. This corresponded to a significant increase of proton pumping activity of plasma membrane vesicles from sucrose-supplied seedlings. A new phosphorylation site was identified in the plasma membrane H^+-ATPase AHA1 and/or AHA2. This phosphorylation site was shown to be crucial for ATPase activity and overrode regulation via the well known C-terminal phosphorylation site. Novel phosphorylation sites were identified for both receptor kinases and cytosolic kinases that showed rapid increases in relative intensities after short times of sucrose treatment. Seven response classes were identified including non-responsive, rapid increase (within 3 min), slow increase, and rapid decrease. Relative quantification of phosphorylation changes by phosphoproteomics provides a means for identification of fast responses to external stimuli in plants as a basis for further functional characterization. ***Molecular & Cellular Proteomics 6:1711–1726, 2007.***

Growth and development of a plant requires precise control and coordination mechanisms of carbon assimilation, transport, and storage. Despite the fundamental importance of these processes (almost all of the organic carbon on earth is derived from them) crucial aspects remain poorly understood. The process of photosynthesis converts CO_2 from the atmosphere to sucrose and starch in leaf cells. Sucrose is exported to supply carbon requirements of other parts of the plant, whereas starch accumulates in the chloroplasts as a transient storage product. At night, conversion of starch storage pools to sucrose maintains the supply of sucrose to non-photosynthetic parts of the plant in the absence of CO_2 assimilation. Thus, transport of sucrose as well as its synthesis and degradation is highly regulated (1–4). Nutrients including sugars also act as signals in all organisms studied so far. For example, yeast has at least three independent pathways involved in glucose signaling: G-protein-coupled receptors, glucose transporter-like sensors, and hexokinase signaling (5).

Similarly in plants, glucose and sucrose are important metabolites and function as signaling molecules, potentially being involved in the regulation of growth and development at the whole plant level (6–9). Although the transcription levels of many genes respond to sugars in general and changes of transcription in response to sucrose depletion and resupply have been globally described (10) with over 100 transcriptional changes after 30 min of sucrose treatment, only a few genes that are regulated by sucrose specifically have been characterized (11). Examples for sucrose-specific responses are the transcription factor ATB2, which is repressed by sucrose at physiological concentrations (12), and the sucrose transporter SUT1 from sugar beet that is regulated by sucrose at the transcriptional level (13). The regulation of sucrose transporter transcription is thought to be mediated via a protein phosphorylation cascade (14). Because hexokinase has been shown to function as a key regulator of glucose-specific responses in plants (15, 16), the question remains how specificity in characteristic sucrose responses may be achieved. Similar to yeast, one may suspect that extracellular sucrose may be directly sensed at the plasma membrane affecting sucrose-specific transport and metabolism. A plasma membrane-localized sucrose sensing mechanism involving sucrose transporters has been suggested in the past (17, 18). Even if the sucrose sensing mechanisms were cytosolic, the responses are likely to involve modulation of sucrose transport at the plasma membrane.

From the ‖Max Planck Institute of Molecular Plant Physiology, Am Mühlenberg 1, 14476 Golm, Germany, ‡Carnegie Institution, Stanford, California 94305, and ¶Department of Plant Biology, University of Copenhagen, Thorvaldsenvej 40, DK-1871 Frederiksberg, Denmark

Received, April 12, 2007, and in revised form, June 1, 2007

Published, MCP Papers in Press, June 23, 2007, DOI 10.1074/mcp.M700164-MCP200

Phosphorylation is the most well known post-translational modification (PTM)[1] involved in signaling. This principle of activation and inactivation of proteins by phosphorylation as well as the function of phosphorylated residues as docking sites for protein scaffolds and complex assembly has been well studied in the field of mammalian signal transduction (19–22). However, most approaches in plant biology so far have been focused on phosphorylation of specific proteins and protein families (23, 24) and the study of specific signaling pathways (25, 26). There have been only a few efforts to globally analyze phosphorylation sites of membrane proteins (27). Although today a vast collection of techniques is available to specifically enrich for and detect phosphorylation sites in plant proteins (28–30), this study is the first that specifically follows phosphorylation events in a plant over time in response to an external stimulus. Such time course studies are of great value for the understanding of phosphorylation during plant signal transduction because they may reveal some important insights into specificity and relevance of individual phosphorylation sites for that given response (31, 32).

In this study, we took a proteomics approach to identify plasma membrane proteins that are phosphorylated in response to sucrose resupply after depletion to *Arabidopsis* seedlings. By quantitative comparison of the relative intensity of phosphoproteins at different times we present first insights into sucrose-induced phosphorylation responses of *Arabidopsis* membrane proteins 3, 5, 10, and 30 min after sucrose resupply. We identified 67 phosphorylation sites of which 70% have not been described before, and we showed sucrose-induced changes in phosphorylation level for 40 of these sites and established *in vivo* roles for some of the responses. The importance of this approach for understanding transporter regulation is demonstrated for a novel phosphorylation site in the C terminus of the AHA proton ATPase, which can override regulation by the well established 14-3-3 autoregulation of activity (33). Importantly receptor kinases also exhibited a change in their phosphorylation status within the first 3 min, suggesting a role close to the core of the signal perception.

EXPERIMENTAL PROCEDURES

Seedling Growth Conditions—*Arabidopsis* (Col-0) seedlings were germinated and grown under constant light (100 μmol m^{-2} s^{-1}) in liquid half-strength Murashige/Skoog medium with 30 mM sucrose for 7 days. After 7 days seedlings were sucrose-starved by changing the medium to half-strength Murashige/Skoog medium without sucrose and placing them in the dark for 24 h to completely starve them for sugars. Sucrose was then resupplied to a final concentration of 30 mM sucrose for 3, 5, 10, and 30 min, respectively, before plant material was harvested for plasma membrane preparation. Seedlings remained in the dark during the sucrose resupply. In a control experiment, 30 mM mannitol was used for resupply.

Plasma Membrane Preparation and Phosphopeptide Enrichment—Plasma membranes of seedlings were isolated using a two-phase partitioning system as described previously (27). Briefly plasma membrane vesicles were inverted using Brij-58, and intracellular protein parts were digested using trypsin. Protein amounts were equalized before tryptic digestion. Protein amounts for each series ranged from 50 to 150 μg between repeated experiments.

Digested peptides were resuspended in 25% acetonitrile and 0.1% TFA and incubated with IMAC resin for phosphopeptide enrichment (PhosSelect, Sigma-Aldrich). Phosphopeptides were eluted from IMAC resin using 400 mM NH_4OH in 25% acetonitrile. Samples were desalted over C_{18} material prior to mass spectrometric analysis (34).

Mass Spectrometric Analysis—Tryptic peptide mixtures were analyzed by LC/MS/MS using nanoflow HPLC (Proxeon Biosystems) and a linear ion trap instrument (LTQ, Thermo Electron) as mass analyzer. Peptides were eluted from a 75-μm analytical column (Reprosil C_{18}, Dr. Maisch GmbH) on a linear gradient running from 10 to 30% acetonitrile in 50 min and sprayed directly into the LTQ mass spectrometer. Proteins were identified by tandem mass spectrometry (MS/MS) by information-dependent acquisition of fragmentation spectra of multiply charged peptides. Zoom scans were implemented after a scan over the full mass range (300–1500 *m/z*) to be able to determine the charge state of the peptides. Additional data-dependent fragmentation (MS3) was used if peptides displayed a loss of phosphoric acid (neutral loss, 98 Da) upon MS/MS fragmentation (35). Fragment MS/MS spectra from raw files were extracted as DTA files and then merged to peak lists using the default settings of DTASuperCharge version 1.17 (SourceForge) with a tolerance of 500 ppm for precursor ion detection. With the default settings, the *m/z* of the respective zoom scans was used as a precursor *m/z* value in the DTA files and peak list. By using the option "Precursor mass N−2," the *m/z* value from the respective zoom scan was assigned to the DTA file and peak lists also for the MS3 fragment spectra.

Fragmentation spectra were searched against a non-redundant *Arabidopsis* protein database (TIGR6, version 2006-09; 30,711 entries; www.arabidopsis.org) using the Mascot algorithm (version 2.1; Matrix Science). The database contains the full *Arabidopsis* proteome and commonly observed contaminants (human keratin, trypsin, and lysyl endopeptidase) so no taxonomic restrictions were applied during automated database search. The following search parameters were applied: trypsin as cleaving enzyme; peptide mass tolerance, 300 ppm; MS/MS tolerance, 0.8 Da; one missed cleavage allowed. Carbamidomethylation of cysteine was set as a fixed modification, and methionine oxidation and phosphorylation of serine, threonine, and tyrosine were set as variable modifications. Only peptides with a length of more than five amino acids were considered. Putative phosphopeptides were manually inspected using the software package MSQuant version 1.4.1 (SourceForge). Peptides were accepted as phosphopeptides if they displayed a neutral loss for serine and threonine phosphorylation or if their fragmentation spectrum displayed b or y ions indicative of phosphorylation.

Phosphorylation site assignment was done using MSQuant version 1.4.1 as described previously (32). Briefly for each peptide different combinations of phosphorylation sites were scored (PTM score), and the highest scoring match was accepted if the sum of the Mascot score and PTM score was higher than 30. If no distinction could be made on this basis, the phosphorylation site was marked as ambiguous.

In general, peptides were accepted without manual interpretation if they displayed a Mascot score greater than 40; peptides with a score greater than 24 were manually inspected, requiring a series of three y or b ions to be accepted. Using the above criteria for protein identification, the rate of false identifications as determined by a search against a reversed TIGR6 *Arabidopsis* database (decoy database)

[1] The abbreviations used are: PTM, post-translational modification; MS3, MS/MS/MS fragmentation; ANOVA, analysis of variance; ABC, ATP-binding cassette; LRR, leucine-rich repeat.

was 1.12%. This was calculated as the percentage of twice the number of "hits" from the decoy database to the total number of hits in both searches (36).

Quantitative Analysis—Within one time series, label-free quantitative analysis of the changes in phosphopeptide intensities was achieved by protein correlation profiling (37). Extracted ion chromatograms of each LC/MS/MS analysis representing different times of sucrose resupply were compared based on their *m/z* values and retention times. Ion intensity sums of *m/z* values identifying the same peptide sequence at the same retention time in different liquid chromatography runs were used for quantitative comparison between the different samples representing different time points.

Label-free relative quantitation of phosphorylation was performed as described previously (38). Briefly for ion intensities of each non-phosphopeptide the deviation from their mean ion intensity across the five time points was calculated. This was performed separately for each peptide species, *i.e.* for each *m/z*. Medians of all relative deviations for peptide species (*i.e.* for each *m/z*) from each protein were then calculated, and outlier peptides were identified based on their significant deviation from the median (χ^2 test). The outlier peptides were excluded from further analysis (see Supplemental Fig. 1). The mean of the remaining non-phosphopeptides was calculated for each time point and used for normalization. Ion intensities of phosphopeptide species (different *m/z*, *i.e.* different charge states treated independently) were normalized against the mean of non-phosphopeptides from the same protein. Subsequently for each phosphopeptide sequence, the mean of normalized intensities was calculated based on the different phosphopeptide *m/z* species, and this value was used to calculate ratios between treated (time points 3, 5, 10, and 30 min) and untreated (time point 0) samples. For each protein only unique non-phosphopeptides were used for normalization.

Peptides conserved in multiple members of a protein family were identified using the "show subsets" option in Mascot, and the respective peptides present in multiple proteins were excluded from quantitative analysis. Also if ion intensities for a given peptide showed signal to noise ratios <2, the respective values were omitted from quantitative analysis. If no unphosphorylated peptides were identified for a given protein, the mean of all identified non-phosphopeptides was used for normalization. These proteins are marked by asterisks in Table II.

Statistical Analysis of Time-dependent Phosphorylation—Within one biological experiment, significance of time-dependent changes in relative phosphorylation was tested by one-way ANOVA using the $\log_2$ ratios of independently quantified analytical replicates. To identify pairwise significant differences between individual time points, one-way ANOVA was combined with a pairwise least significant difference test. Time series effects were considered as significant if $p < 0.05$. Statistic operations were carried out using the "Analyze-it" Excel add-on version 1.73.

The time series experiment of sucrose depletion and resupply was repeated in three independent biological experiments, and two of the experiments were suitable for quantitative analysis. One additional experiment was carried out with carbon depletion and mannitol resupply. If not stated otherwise, mean $\log_2$ ratios ±S.D. from analytical replicates of the experiment with the most quantified phosphopeptides are presented. Reproducibility of the time course responses between two biological experiments was confirmed by linear regression analysis ($r^2 = 0.725$; $p < 0.01$) of the $\log_2$ ratios of quantifiable phosphopeptides identified in both of the two independent experiments across all time points (Supplemental Fig. 2).

Cluster analysis of the responses was done using Ward's method of increase in the sum of squares as a measure using ClustanGraphics version 8. For a given classification, the increase in the sum of squares of all cases in that classification is the minimum. The clustering method is tolerant for missing values.

Constructs for Expression of Arabidopsis AHA2 in Saccharomyces cerevisiae—A centromeric yeast expression vector (pMP1733) containing the PMA1 promoter was used for expression of different versions of the *AHA2* gene. *aha2T881A* and *aha2T947A* mutant genes (33) were transferred to this expression vector by inserting XhoI-SpeI fragments from pMP720 and pMP832, respectively. The *aha2T947D* mutation was generated by insertion of a linker containing the mutation into a SacI-SpeI-digested vector containing the *AHA2* gene (pMP1745). The *aha2T881D* mutant was generated by polymerase chain reaction-assisted cassette mutagenesis in which an ApaI-SacI fragment containing the desired mutation was inserted into ApaI-SacI-digested pMP1745. All mutations were confirmed by sequencing.

Yeast Complementation Tests—*S. cerevisiae* strain RS-72 (*Mat a; ade1-100 his4-519 leu2-3,312 pPMA1::pGAL1*) was used for complementation tests (39). The experiment was replicated independently three times with cells from independent transformation events. Isolation of plasma membrane protein from the yeast strain RS-72 was performed essentially as described previously (33).

Measurement of Proton Transport by the ATPase—Proton transport was assayed as described previously (40) by monitoring fluorescence quenching of 9-amino-6-chloro-2-methoxyacridine, a dye that upon protonation accumulates in an impermeant form inside vesicles. The initial decrease in fluorescence is therefore a direct effect of the amount of protons transported into the plasma membrane vesicles by the H^+-ATPase. The reaction medium contained 20 mM MOPS-KOH, pH 7.0, 1 mM ATP, 40 mM K_2SO_4, 25 mM KNO_3, and 60 nM valinomycin. The assay were performed in a volume of 2.4 ml using 8 μg of plasma membrane protein. The reaction was started by addition of 2 mM $MgSO_4$. Protein concentrations were determined by the method of Bradford with the Bio-Rad protein assay reagent and γ-globulin as a standard.

Overlay Assays and Western Blots—SDS-PAGE, Western blotting, and 14-3-3 overlay assays were performed as described previously (41). Briefly equal amounts of plasma membrane protein were loaded on a regular SDS gel, blotted to a nitrocellulose membrane, and incubated with $MRGSH_6$-tagged GF14-ω 14-3-3 protein. Bound 14-3-3 protein was subsequently detected immunologically using a primary anti-$RGSH_6$ antibody (Qiagen) followed by incubation with a secondary anti-IgG antibody conjugated with alkaline phosphatase. For detection of H^+-ATPase antibodies raised against either the N terminus (number 762) or C terminus (number 759) of plasma membrane H^+-ATPase were used (1:5000) (42).

RESULTS

Isolation of Plasma Membrane Phosphopeptides—To determine the effect of sucrose on phosphorylation of plasma membrane proteins, *Arabidopsis* seedlings were germinated and grown in continuous light in liquid Murashige/Skoog medium supplemented with 30 mM sucrose for 7 days. The growth medium was replaced by sugar-free medium, and seedlings were kept in darkness for 24 h. Subsequently sucrose was added to the medium to a final concentration of 30 mM in darkness. Plasma membranes were isolated by two-phase partitioning, and inside-out vesicles were generated by treatment with 0.02% Brij-58 and digested with trypsin (27). Phosphopeptides were enriched by IMAC and were subjected to LC/MS/MS analysis. The contamination from endomembranes, chloroplasts, and mitochondria in the plasma membrane preparation was estimated to be ~19%, which is in agreement with experimentally determined contamination of plasma membrane preparations using stable isotope labeling (43).

TABLE I
List of identified proteins with transport functions

The number of identified unique peptides refers to peptides with different sequences. The accession numbers refer to the *Arabidopsis* Gene Identifier (AGI) codes (*Arabidopsis* protein database, www.arabidopsis.org).

Transport function	AGI code	Protein name	Unique peptides	Sequence coverage
				%
Plasma membrane ATPases	At2g18960	AHA1	46	4.8
	At3g47950	AHA4	2	1.2
	At3g60330	AHA7	5	0.9
	At4g11730	AHA12	2	1.2
	At4g30190	AHA2	34	11.8
	At5g57350	AHA3	3	1.3
	At5g62670	AHA11	10	1.5
Ca^{2+}-transporting ATPase	At5g57110	ACA8	6	2.8
Peptide transporters	At1g52190		6	1.0
	At3g54140	PTR1	2	0.7
	At4g16370	OPT1	4	1.5
	At5g62680		2	1.2
ABC transporters	At1g59870	PDR8/PEN3	14	1.0
	At2g07680	MRP13/MRP11	2	1.1
	At2g47000	PGP4/MDR4	10	1.8
	At3g62150	PGP21/MDR17	15	7.0
Potassium channels	At2g40540	KT2	2	1.3
Monosaccharide transporters	At1g11260	STP1	7	20.7
	At3g18830	PLT5	5	0.9
	At3g19930	STP4	2	1.4
	At4g02050	STP7	4	1.3
	At5g26340	STP13	2	1.1
Sucrose transporter	At1g71880	SUC1	4	1.8
Sulfate transporters	At1g23090	Sultr3.3	3	0.5
	At4g02700	Sultr3.2	2	0.1
Phosphate transporters	At2g38940	PT2/PHT1-4	5	0.9
	At5g43350	PT1/PHT1-1	5	1.0
Aquaporins	At2g37170	PIP2.2	4	1.4
	At2g39010	PIP2.6	5	1.7
	At4g23400	PIP1.5	2	0.5
	At3g53420	PIP2.1	2	0.4
	At2g45960	PIP1.2	2	0.7

The majority of proteins (36%) identified from *Arabidopsis* seedling plasma membrane preparations in all experiments were transport-related. These included seven isoforms of the plasma membrane proton ATPase family, five aquaporins, four peptide transporters, four ABC transporters, five monosaccharide transporters, one sucrose transporter, and two phosphate and sulfate transporters (Table I). The second largest functional category with 12% of identified proteins consisted of membrane-anchored proteins involved in cell wall architecture, such as glycosylphosphatidylinositol-anchored proteins. Roughly 10% of all identified peptides belonged to proteins with yet uncharacterized functions.

Among the peptides found to be phosphorylated upon sucrose treatment, the fraction of proteins with protein modifying activities (9%), signaling proteins (12%), and receptor kinases (17%) was increased significantly compared with their fraction in all identified tryptic peptides (Fig. 1). This indicates that protein modification and especially kinases indeed have important roles during perception and uptake in response to sucrose supply after 24 h of sugar deprivation. A full list of all identified phosphopeptides is presented in Table II.

Sugar-induced Regulation of Plasma Membrane H^+- and Ca^{2+}-ATPases—Plasma membrane H^+-ATPases represent the most abundant fraction of peptides identified, confirming results from previous phosphoproteomics studies in *Arabidopsis* cell suspension cultures (27, 30). In total, seven isoforms of plasma membrane H^+-ATPases were identified in seedlings as concluded from the unambiguous identification of two or more specific tryptic peptides for each protein. Among the seven isoforms, the two most well characterized plasma membrane H^+-ATPases, AHA1 and AHA2, were the most abundant isoforms, *i.e.* the most peptides were identified for these proteins (Table I).

Activation of the H^+-ATPase provides the driving force for proton-coupled transport processes (*i.e.* sucrose transport). Therefore, it is not surprising to find phosphopeptides of the most abundant ATPases AHA1 and AHA2 as highly responsive to sucrose treatment (Table II). The relative ion intensity of

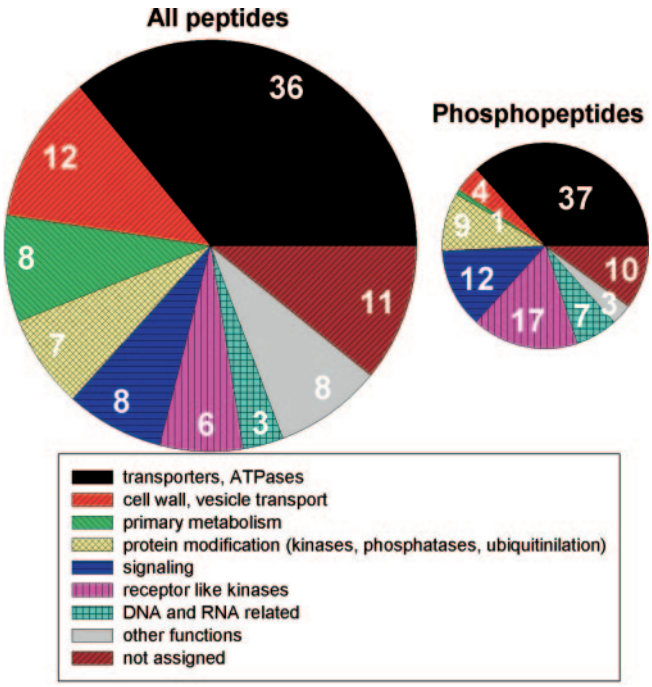

FIG. 1. **Pie charts of functional categories of the proteins identified by the total number of tryptic peptides (961 unique peptides) and for phosphopeptides (67 unique peptides) in all experiments.** The fraction of peptides identifying proteins with modifying functions, signaling proteins, and receptor kinases is higher among the phosphopeptides. *Area* of *pie charts* represents total number of peptides in each category.

the phosphopeptides GLDIDTAGHHYpTV (where pT is phosphothreonine) and GLDIETPSHYpTV representing Thr-947 in AHA1 and AHA2 increased with increasing duration of the sucrose resupply and reached highest ratios after 30 min of sucrose resupply (Table II and Fig. 2*A*). The C-terminal 14-3-3 protein-binding site (peptides GLDIDTAGHHYpTV and GLDIETPSHYpTV) is well conserved, and this phosphorylation site is known to be essential for the regulation of proton pumps by interaction of a 14-3-3 protein with the phosphorylated threonine (41, 44, 45).

Proton pumping activity of plasma membrane vesicles of sucrose-supplied seedlings significantly ($p < 0.01$) increased after 30 min compared with plasma membrane vesicles from sucrose-depleted seedlings (Fig. 2*B*). This finding correlates well with the observed increase in phosphorylation of the C-terminal regulatory site at Thr-947 (Fig. 2*A*) and supports the quantitation approach. Furthermore in an overlay assay we were able to demonstrate that phosphorylation-dependent 14-3-3 binding to similar levels of ATPase was significantly stronger in sucrose-treated plasma membranes (Fig. 2*C*). This provides additional support for sucrose-dependent changes in phosphorylation and activation of the proton pumps.

Another phosphopeptide for ATPases, pTLHGLQPK, identifies a previously undescribed phosphorylation site also in the C terminus of AHA1 and AHA2 at Thr-881. Because the peptide pTLHGLQPK is identical between AHA1 and AHA2, we cannot distinguish which of the two proton ATPase isoforms contributes more to the phosphorylation of pTLHGLQPK, and the observed time course of phosphorylation change is an overlay of the response in both proteins (Table II). The phosphorylation site pTLHGLQPK was clearly identified by neutral loss and subsequent MS3 fragmentation (Fig. 3*A*). By expressing site-directed mutants of this phosphorylation site in yeast, we were able to show that this site, Thr-881, is crucial for plasma membrane ATPase activity in AHA2. In a yeast mutant deficient in the endogenous plasma membrane H^+-ATPase, *pma1*, expression of AHA2 to a limited degree complemented growth. When placed on medium containing galactose, the yeast endogenous H^+-ATPase *PMA1* was expressed. When grown on medium containing glucose as the single carbon source, plant H^+-ATPase isoforms will be expressed only, and the growth of the yeast cells is dependent on the activity of the plant H^+-ATPase. Thr-881 and Thr-947 were mutated into Asp and Ala to study the effect of a negative charge at these positions. Strikingly if Thr-881 was mutated to Asp, thus mimicking phosphorylation, growth was stimulated markedly and was comparable to growth of the *pma1* mutant complemented with a mutant of AHA2 (aha2Δ92) completely devoid of its autoinhibitory C-terminal domain (Fig. 3*B*). Mutation of Thr-881 to Ala inhibited the growth rate of transformed cells. The fact that mutating Thr-881 to an Asp resulted in pump activation suggests that phosphorylation of Thr-881 directly produces an activated pump without the need for additional protein partners such as 14-3-3 proteins. The phosphorylation site at Thr-881 of AHA1 and AHA2 is homologous to the peptide pTLHGLQAPDAK representing Thr-889 in the C terminus of the plasma membrane ATPase AHA11, and this phosphorylation site is conserved in all 12 members of the plasma membrane ATPase family except for AHA10 and AHA12.

Thr-947 was likewise mutated to Asp and Ala, respectively. Neither mutation had a stimulatory effect on yeast growth (Fig. 3*B*) even though both mutant proteins were expressed to the same level as the C-terminally truncated pump (Fig. 3*C*). This was not unexpected because activation by phosphorylation of Thr-947 requires subsequent binding of 14-3-3 protein to produce activation of the pump. Because Asp is very different in size compared with phosphate it might not fit into the binding groove of the 14-3-3 protein (46). Examination of the C-terminal regulatory domain of AHA2 provides a likely explanation for the functional differences between phosphorylation of Thr-881 and Thr-947. Thus, Thr-881 is situated in a stretch of amino acid residues important for negative regulation of the H^+-ATPase (previously defined as autoinhibitory Region I (33)), whereas Thr-947 is not included in any of the two autoinhibitory regions of the pump. It can therefore be hypothesized that introducing a negative charge in autoinhibitory Region I directly abolishes the interaction of the C-terminal regulatory domain with the rest of the protein. Thus, the

TABLE II

List of all 67 phosphopeptides identified from plasma membrane preparations of Arabidopsis seedlings starved and resupplied with sucrose in three independent experiments

In those cases in which the site of phosphorylation could be determined, it is noted by pS for phosphoserine, pT for phosphothreonine, or pY for phosphotyrosine. Ambiguities are indicated by small letters in parentheses. The peptides for which quantitative information was retrieved are shown in bold (displayed in figures) or in italics (not in figures), and the normalized intensity ratios of phosphopeptides to non-phosphopeptides are shown. For proteins marked with asterisks, only phosphopeptides were identified. Time-dependent responses are considered as significant if $p < 0.05$ as determined by one-way ANOVA. AGI, *Arabidopsis* Gene Identifier; AA, amino acid; GAP, GTPase-activating protein; BRCT, BRCA1 C terminus; oxM, oxidized methionine.

Accession (AGI code)	Description	Sequence with modifications		0	3	5	10	30	Mascot score	*m/z*	Charge	Modification	Left AA	Right AA	Relative mass error	*p* (one-way ANOVA)
															ppm	
Sucrose responses																
At2g18960	Plasma membrane proton ATPases (AHA1 and AHA2)	**pTLHGLQPK**		0.00	−0.66	−0.02	−0.26	0.04	52	973.38	1	1pT	Arg	Glu	−122.52	0.21
At2g18960	Plasma membrane proton ATPase (AHA1)	**GLDIDTAGHHYpTV**		0.00	0.93	0.14	1.72	2.88	53	739.67	2	1pT	Lys	—[a]	−171.49	0.01
At4g30190	Plasma membrane proton ATPase (AHA2)	**GLDIETPSHYpTV**		0.00	0.26	1.04	−0.11	1.46	58	706.10	2	1pT	Lys	—	−257.39	0.03
At5g57110	Ca^{2+}-transporting ATPase ACA8	**pSEHADSDSDTFYIPSK**		0.00	−0.38	−0.88	−0.14	−0.29	44	939.85	2	1pS	Lys	Asn	−40.873	0.04
At5g62670	Plasma membrane proton ATPase (AHA11)	pTLHGLQAPDAK							32	616.09	2	1pT	Arg	Met	148.469	
At1g52190	Peptide transporter	**GFEKEDLpSPVVK**		0.00	−0.55	−0.36	−0.28	−0.61	60	714.15	2	1pS	Lys	Thr	−232.97	0.24
At1g59870	Putative ABC transporter	MpSNELAVPFDK							26	444.13	3	1pS	Lys	Ser	338.244	
At1g59870	Putative ABC transporter	*SLpSTADGNR*		0.00		−0.41	−0.22		34	500.50	2	1pST	Arg	Arg	−276.86	
At1g61250	Secretory carrier membrane protein (SC3)	*LpSPLPPEPVGFDYGR*		0.00	0.18	−0.30	0.00	−0.04	36	862.65	2	1pS	Arg	Thr	280.152	0.66
At1g71880	Sucrose transporter SUC1	**DAAALETQpSPEDFDQPSPLR**		0.00	−0.41	−0.46	−0.29	0.40	42	1133.78	2	1pS	Lys	Lys	−231.92	0.12
At2g37170	Aquaporin PIP2b	**SLGpSFR**		0.00	0.23	0.36	0.23	−0.17	27	373.69	2	1pS	Lys	Ser	118.689	0.57
At2g37170	Aquaporin PIP2b	SLGpSFRpSAANV							24	634.60	2	2pS	Lys	—	−173.62	
At2g39010	Aquaporin PIP2e	**pSQLHELHA**		0.00	−0.62	1.19	0.60	−1.75	35	507.57	2	1pS	Arg	—	−175.62	0.00
At2g39010	Aquaporin PIP2e	*TKDEL(t)EEE(s)L(s)GK*		0.00	−0.54	−0.34	0.25	0.35	75	864.22	2	2pST	Met	Asp	−188.4	0.11
At2g39480	Putative ABC transporter	*RQDpSFEMR*	*						30	574.59	2	1pS	Lys	Leu	−160.9	
At4g18910	Major intrinsic protein-like	SGpSFLK	*						33	359.59	2	1pS	Lys	Thr	134.752	
At1g22280	Protein phosphatase type 2C-like protein	*TDQAIL(s)N(ss)DLGR*		0.00	−0.34	0.02	−0.17	−0.71	53	779.12	2	1pS	Lys	Gly	370.183	0.16
At3g01490	Protein kinase-like protein	**(s)L(s)DGEDNVNNTR**	*	0.00	−0.81	−0.42	1.28	0.62	33	750.57	2	1pS	Lys	His	−278.9	0.02
At3g45780	Nonphototropic hypocotyl 1 (NPH1)	**(ss)GEMSDGDVPGGR**		0.00	−0.08	0.36	0.52	0.19	38	715.59	2	1pS	Arg	Ser	−207.24	0.47
At3g45780	Nonphototropic hypocotyl 1 (NPH1)	FLQG(s)G(t)DADELAK							28	726.16	2	1pST	Arg	Ile	57.9872	
At4g19930	F-box family protein	VPpSFIQR	*						28	463.59	2	1pS	Arg	Leu	−152.46	
At4g35230	Protein kinase family protein	**SYpSTNLAYTPPEYLR**		0.00	0.17	0.24	0.74	0.56	46	927.55	2	1pS	Lys	Asn	−405.11	0.40
At4g35600	Protein kinase family protein	**VGpSGMIVAIK**	*	0.00	−0.04	0.74	−0.02	0.22	41	527.93	2	1pS	Arg	Arg	117.738	0.23
At5g41260	Protein kinase-like	**pSNPDVTGLDEEGR**		0.00	−0.14	−0.95	0.33	−0.14	42	735.15	2	1pS	Arg	Gly	303.797	0.05
At5g41260	Protein kinase-like	**SYpSTNLAFTPPEYLR**		0.00	0.95	0.84	0.36	0.53	34	919.68	2	1pS	Lys	Thr	−269.11	0.05
AtCg00860	ycf2.1 hypothetical protein	WYFELG(ts)MKK							26	517.13	3	pST	Lys	Phe	97.215	
At1g05150	Putative *O*-GlcNAc-transferase	*DNDVPV(s)Y(s)GSGGPTK*		0.00	0.64	0.89	0.99	0.14	34	830.62	2	1pS	Arg	Ser	333.23	0.21

TABLE II—*continued*

Accession (AGI code)	Description	Sequence with modifications		0	3	5	10	30	Mascot score	*m/z*	Charge	Modification	Left AA	Right AA	Relative mass error	*p* (one-way ANOVA)
															ppm	
At1g19870	Calmodulin-binding family protein	*KVpSNPSFIAAQSK*		0.00	−0.52	−0.13	0.32	−0.35	40	728.70	2	1pS	Arg	Phe	−186.24	0.16
At1g19870	Calmodulin-binding family protein	VEPEE(s)E(s)DDVIIVR							34	898.18	2	1pS	Lys	Lys	−253.37	
At1g74690	Calmodulin-binding family protein	*SGGMLETQNVGPEEIpSDDEI-ELPEGK*	*	0.00	−0.08	0.21	0.66	0.50	30	952.05	3	1pS	Arg	Ser	303.188	0.32
At3g50840	Phototropic-responsive NPH3 family protein	VIL(s)MK(ss)VLSPEIVER							24	983.89	2	1pS	Arg	Ser	185.175	
At5g37710	Calmodulin-binding heat-shock protein like	*(s)N(s)GEFVLNDNVVPER*		0.00	0.23	0.38	0.79	0.39	55	928.67	2	1pS	Arg	—	261.906	0.56
At5g45750	Rab-type small GTP-binding protein-like	HSpTFENVETWLKELR							24	683.52	3	1pT	Arg	Asn	115.35	
At5g61530	Small G protein family protein/RhoGAP	VGSLFKpSR							50	487.14	2	1pS	Arg	Trp	58.8691	
At1g16120	Wall-associated kinase	EVpSNELER							28	528.08	2	1pS	Lys	Ile	98.3942	
At1g53730	LRR receptor-like protein kinase (SRF6)	*NKpSFDDEDSTR*	*	0.00	0.80	−0.13	−0.43	−0.47	54	697.09	2	1pS	Arg	Lys	−211.8	0.04
At3g02880, At5g53320, At5g16590, At4g23740, At3g08680, At5g05160, At3g17840, At5g58300, At1g48480, At2g26730	Receptor-like kinase LRR III	*ApSAEVLGK*		0.00	−0.27	−0.33	0.24	0.05	50	427.56	2	1pS	Lys	Gly	−152.15	0.39
At3g02880	Receptor-like kinase LRR III	*LIEEVSHSSG(s)PNPV(s)D*		0.00	−0.33	−0.35	−0.30	−1.37	37	917.14	2	1pS	Arg	—	−285.8	0.01
At3g14350	LRR receptor-like protein kinase (SRF7)	**HKpSFDDDDSTMR**		0.00	0.79	−0.17	−0.09	0.75	64	767.08	2	1pS	Arg	Lys	−242.19	0.03
At5g10020	Receptor-like kinase LRR III	*FSDQPVMLDVYpSPDR*	*	0.00	0.85	−0.78	−0.30	−0.32	59	925.27	2	1pS	Arg	Leu	391.221	0.05
At5g58300	Receptor-like protein kinase	SPVQ(s)P(s)RDDMVDLPR							29	627.14	3	1pS	Lys	Trp	130.953	
At1g11960	Early responsive to dehydration protein-related	(ss)PLHSGALVSK							34	631.64	2	1pS	Arg	Phe	−198.18	
At3g28860	ABC transporter	*NLSY(sy)STGADGR*		0.00	−0.75	−0.62	−0.52	−0.26	58	735.85	2	1pY 1pS	Arg	Ile	105.75	0.12
At1g53300	Thioredoxin family protein	(ssst)VATGETPIWK							22	772.14	2	1pST	Arg	Lys	195.61	
At1g53300	Thioredoxin family protein	IQI(t)GM(t)QSR							24	608.10	2	1pT	Lys	Ser	140.076	
At3g52400	Syntaxin-like protein synt4	*ANpSLVR*	*	0.00		−0.23	−0.38	−0.71	29	370.00	2	1pS	Arg	Ser	−239.01	0.17
At4g31480	Coatomer β subunit	AVNpYLLpSNVDK							21	466.13	3	1pY 1pS	Arg	Val	55.4827	
At5g38190	Myosin heavy chain-related	MG(sss)PNNSVDSYIR							24	565.05	3	1pS	—	Glu	316.743	
At2g20330	Putative WD-40 repeat protein	IWDVNNFL(s)Q(t)QVIKPK	*						24	705.05	3	1pST	Arg	Leu	195.61	
At3g48740	MTN3-like protein	*LGTV(ss)PEPISVVR*		0.00	0.52	−0.25	−0.48	0.12	46	760.93	2	1pS	Lys	Gln	75.4427	0.18
At1g22530	SEC14 cytosolic factor family protein	*(y)GGL(s)K_D(s)PF(t)VEDGVTE-AVVK*		0.00	−0.91	−0.01	−2.97	−0.23	47	846.50	3	1pY 2pST	Lys	Ser	−210.04	0.00

TABLE II—*continued*

Accession (AGI code)	Description	Sequence with modifications		0	3	5	10	30	Mascot score	*m/z*	Charge	Modification	Left AA	Right AA	Relative mass error	*p* (one-way ANOVA)
															ppm	
At2g13940	Putative retroelement pol polyprotein	AQL(ss)CRQDGQAVIEYYGR							28	556.67	4	1pS	Arg	Leu	−109.34	
At4g04430	Putative transposon protein	GYNRpSMQVpYNWDR	*						24	617.66	3	1pY 1pS	Lys	Ser	88.4223	
At2g45820	Remorin	ALAVVEKPIEEHpTPKK	*						34	623.49	3	1pT	Lys	Ala	−206.59	
At3g61260	Remorin	*LpSFVR*	*	0.00	−1.69	−1.06	−1.00	−0.54	25	351.04	2	1pS	Arg	Ala	−113.25	0.00
At5g24470	Pseudo-response regulator 5 (APRR5)	NEDGYSLpSVGK							24	417.19	3	1pS	Lys	Ile	49.1971	
At1g23870	Glycosyltransferase family 20 protein (AtTPS9)	KETYpSTAK							26	504.08	2	1pS	Lys	Arg	243.512	
At1g15400	Unknown protein	(tt)GRV(s)PAVDPP(s)PR							24	848.61	2	1pT	Arg	Ile	−301.2	
At1g15400	Unknown protein	QG(ss)GIVFDDR	*						36	630.66	2	1pS	Arg	Leu	102.587	
At1g15400	Unknown protein	**VpSPAVDPPpSPR**		0.00	−0.72	−1.00	−0.12	0.03	33	641.10	2	2pS	Arg	Ile	−194.43	0.03
At3g22390	Unknown protein	KpSGGGAIGK							35	854.23	1	1pS	Arg	Thr	78.1825	
At3g25070	RPM1-interacting protein 4 (RIN4)	*pSREESELK*		0.00		−0.70	−0.51	−0.74	63	507.57	2	1pS	Arg	Gln	65.4766	
At3g25070	RPM1-interacting protein 4 (RIN4)	*ADEpSPEKVTVVPK*	*	0.00	−1.14	−0.85	−0.24	−1.26	46	739.75	2	1pS	Arg	Phe	−113.18	0.01
At4g02110	BRCT domain-containing protein	VpSAPVTGNSNQK							28	641.04	2	1pS	Lys	Glu	203.683	
At4g32285	Epsin N-terminal homology (ENTH) domain-containing	*pSFGDVNEIGAR*	*	0.00	−0.37	0.05	0.03	0.08	58	623.07	2	1pS	Arg	Glu	261.701	0.57
At5g45510	Leucine-rich repeat family protein	**KEDpTDGEDEIR**	*	0.00	−0.82	−1.02	−0.39	−0.16	39	693.61	2	1pT	Lys	Ser	−189.76	0.03
At5g50101	Unknown protein	AIQGTSTDPVIpTPLK	*						34	810.52	2	1pT	Arg	Asn	−48.373	
Mannitol responses																
At2g18960	Plasma membrane proton ATPase (AHA1)	GLDIDTAGHHYpTV		0.00	0.99	1.23	1.42	1.50	39	739.81	2	1pT	Lys	—	−0.3065	0.02
At2g18960	Plasma membrane proton ATPases (AHA1 and AHA2)	pTLHGLQPK		0.00	−0.06	−0.10	−0.26	−0.23	26	487.24	2	1pT	Arg	Glu	−0.6981	0.88
At4g30190	Plasma membrane proton ATPase (AHA2)	GLDIETPSHYpTV		0.00	0.13	0.22	−0.07	0.24	47	706.31	2	1pT	Lys	—	2.77478	0.44
At1g57990	Purine permease-related	QTTAEGSANPEPDQILpSPR	*	0.00	−0.12	−0.49	−0.41	−0.34	58	1045.97	2	1pS	Lys	Arg	−0.4627	0.45
At2g39010	Aquaporin PIP2e	pSQLHELHA		0.00	0.33	0.70	−0.23	−0.13	18	507.72	2	1pS	Arg	—	−2.6667	0.24
At1g19870	Calmodulin-binding family protein	VEPEEpSESDDVIIVR		0.00	0.24	−0.13	0.31	0.34	47	898.40	2	1pS	Lys	Lys	−0.1621	0.59
At3g01830	Calmodulin-related protein, putative	oxMLSLLGEpSKpSLK	*	0.00	0.44	0.36	0.68		26	741.34	2	2pS, 1oxM	Arg	Asp	4.11399	0.47
At3g08510	Phosphoinositide-specific phospholipase C (PLC2)	EVPpSFIQR		0.00	0.31	0.24	0.04	0.10	28	528.24	2	1pS	Arg	Asn	−2.298	0.49
At4g19930	F-box family protein	VPpSFIQR		0.00	0.53	−0.03	0.18		30	463.72	2	1pS	Arg	Leu	−0.3695	0.08
At3g02880	Receptor-like kinase LRR III	ApSAEVLGK							17	427.70	2	1pS	Arg	Gly	−1.2259	
At3g02880	Receptor-like kinase LRR III	LIEEVSHSSG(s)PNPV(s)D		0.00	−0.17	−0.38	−0.33	−0.31	27	917.39	2	1pS	Arg	—	0.01691	0.28
At5g37970	*S*-Adenosyl-L-methionine: carboxyl methyltransferase	pYVNYFIVLKR		0.00	0.03	−0.30	0.14	0.05	22	697.86	2	1pY	Lys	Lys	−3.6159	0.15
At3g08710	Thioredoxin family protein	VTSIIDSVPEpSPQRP		0.00	0.00	0.05	−0.16		58	852.91	2	1pS	Lys	—	−2.5442	0.65
At3g50280	Transferase family protein	ELpSPTFKER	*	0.00	0.99	1.13	1.79		22	593.77	2	1pS	Arg	Val	−1.0641	0.00

TABLE II—*continued*

Accession (AGI code)	Description	Sequence with modifications		0	3	5	10	30	Mascot score	*m/z*	Charge	Modification	Left AA	Right AA	Relative mass error	*p* (one-way ANOVA)
															ppm	
At3g48740	MTN3-like protein	LGTV(ss)PEPISVVR		0.00	0.84	0.53	0.17		44	760.88	2	1pS	Lys	Gln	1.60673	0.03
At3g61260	Remorin family protein	IALEpSESPAK	*	0.00	0.55	0.81	1.34		40	562.76	2	1pS	Lys	Val	−0.9126	0.01
At3g61260	Remorin family protein	LpSFVR		0.00	−0.60	−0.21	−0.08	0.12	24	351.16	2	1pS	Arg	Ala	−3.0481	0.04
At1g21580	Hydroxyproline-rich glycoprotein family protein	SLGpYAR		0.00		−2.36	−1.74		17	373.66	2	1pY	Arg	Lys	−1.2458	
At1g62060	Expressed protein	QVEEVSKEpTK		0.00	−0.36	0.14	0.34		21	628.78	2	1pT	Arg	Leu	−10.708	0.28
At1g66480	Expressed protein	LDoxMLMLpSR		0.00	0.44	0.60	0.20		25	537.74	2	1pS, 1oxM	Arg	Arg	6.81652	0.48
At3g20110	Cytochrome P450 family protein	LREEIDpSVVGETR		0.00	0.31	0.24	0.04	0.01	23	528.24	3	1pS	Arg	Leu	−9.9737	0.35
At4g32285	Epsin N-terminal homology (ENTH)	pSFGDVNEIGAR		0.00	0.17	0.18	0.17	0.19	31	622.76	2	1pS	Arg	Glu	1.1157	0.86
At4g39530	Pentatricopeptide (PPR) repeat-containing protein	ASASLTSLGLpSK		0.00		0.68			17	607.80	2	1pS	Arg	Gln	−2.6624	

[a] — indicates that there is no further amino acid in the sequence, *i.e.* if the tryptic peptide was the C- or N-terminal peptide of that protein.

two sites are independent of each other, and the proton pump can become activated by phosphorylation at either site, and further phosphorylation at the other site would produce an additive effect. The Thr-881 phosphorylation site is in autoinhibitory Region I, and phosphorylation at this site activates the pump directly. The Thr-947 site is downstream of autoinhibitory Region II, and phosphorylation at this site has to be followed by 14-3-3 binding to produce activation.

A plasma membrane Ca^{2+}-transporting ATPase (ACA8; At5g57110) displayed a decrease of phosphorylation at Ser-22 (Table II and Fig. 4*A*) after 5 min. The N-terminal region of type II B calcium-ATPases (such as ACA8) is known to have regulatory functions through a calmodulin-binding site, an autoinhibitory domain covering also Ser-22, and through phosphorylation (47). Phosphorylation of Ser-45 in the N terminus of ACA2 was shown to reduce calmodulin stimulation of ACA2 (48).

Sucrose Transporters—A phosphorylation site was identified for the sucrose transporter SUC1 at Ser-20 in the N-terminal part of the protein. The relative intensity of this phosphopeptide slightly increased after 30 min of sucrose supply (Table II and Fig. 4*A*). Although phosphorylation of sucrose transporters has been suggested in the past, this is the first conclusive identification of a site of phosphorylation in the sucrose transporter family (see Supplemental Fig. 3). The N terminus of sucrose transporter AtSUC5 was also found to be phosphorylated at a similar peptide, but there the precise site of phosphorylation was not resolved (27). In fact all *Arabidopsis* sucrose transporters except AtSUC2 contain this serine as a conserved potential phosphorylation site in their N terminus. This suggests that N-terminal phosphorylation may be a common way to regulate sucrose transporter activity or affinity. It was suggested from studies involving phosphatase inhibitors that sucrose transporter activity is regulated by phosphorylation (14, 49), and studies using chimeric sucrose transporter constructs suggest that the N terminus is regulating the affinity of sucrose transport (50). Similarly for the H^+/ATPase, functional studies in yeast as well as in plants promise to provide insights into the post-translational regulation. It is interesting to note that sucrose transporter protein has a high turnover, and phosphorylation may provide a means for regulating activity at the post-translational level (51).

Aquaporins—Three phosphorylation sites were found for aquaporins (Table II and Fig. 4*A*). Aquaporin PIP2e was found to be phosphorylated in the N-terminal peptide TKDELTEEESLSGK and at Ser-282 (pSQLHELHA where pS is phosphoserine). A phosphorylation site of aquaporin PIP2b was found at Ser-278 (SLGpSFR). Phosphorylated Ser-278 and Ser-281 in PIP2b are among the two conserved serine residues that control pore gating. Upon dephosphorylation, the pore is closed (52). Interestingly Ser-278 appears to locate the C-terminal domain, which interacts with the neighboring subunit of the tetramer. This finding may suggest that PIP2 aquaporins use an allosteric trans-regulatory mechanism for

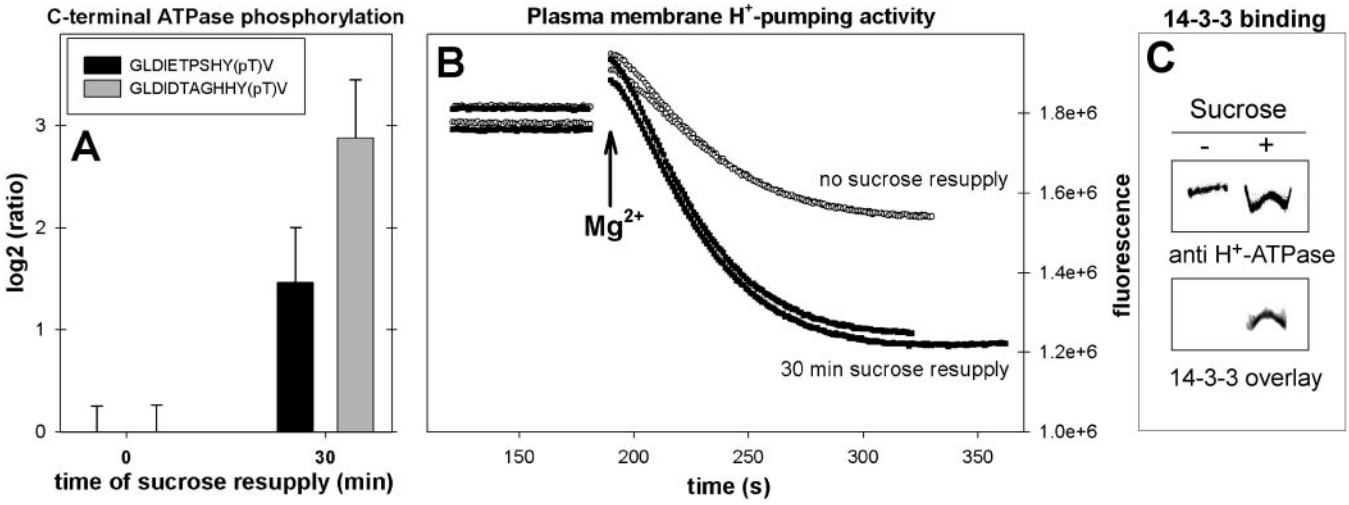

FIG. 2. **Regulation and activity of plasma membrane ATPases.** *A*, relative phosphorylation of the C-terminal phosphorylation sites for AHA2 and AHA1 displayed 30 min after sucrose resupply. *B*, proton pumping measured by the quenching of 9-amino-6-chloro-2-methoxy-acridine fluorescence. Plasma membranes containing the H^+-ATPase were incubated with ATP, and proton pumping was activated by addition of magnesium. The initial decrease in fluorescence was a direct effect of the amount of protons transported into the vesicles by the H^+-ATPase. The experiment shows two repetitions using 8 μg of the same purification of plasma membranes. *C*, binding of 14-3-3 protein to plasma membrane H^+-ATPase is increased upon sucrose treatment of seedlings. Plasma membrane (4 μg) from *Arabidopsis* seedlings was subjected to SDS-PAGE and transferred to a nitrocellulose membrane. *Upper panel*, Western blot detecting the H^+-ATPase C terminus. *Lower panel*, 14-3-3 binding in an overlay assay. The H^+ pumping and 14-3-3 binding experiments were repeated on three independently plasma membrane purifications.

rapid shutoff as recently found in AMT ammonium transporters (53). The phosphorylation site at Ser-282 in PIP2e is in a conserved position homologous to the regulatory Ser-281 of PIP2b and may well have regulatory function also in PIP2e. The time course of Ser-282 at PIP2e displays a significant increase of relative phosphorylation after 5 min and a strong decrease after 30 min (Fig. 4*A*), suggesting that addition of external sucrose leads to a rapid transient opening of the PIP2e pore and a subsequent adaptation response with pore closing. Possibly adjustments to osmotic changes are involved in these processes. The role of the N-terminal phosphorylation site of PIP2e remains unclear especially because it did not show a strong response to sucrose. Phosphorylation of the aquaporin PIP2b showed only slight response to sucrose resupply (Fig. 4*A*).

Protein Kinases—Because the receptors and signaling cascades for the sugar responses are not known in plants, the identification of receptors as candidates for involvement in sucrose responses is of major interest. In total, 34 receptor-like kinases were identified with more than two tryptic peptides. Among these, six were found to be phosphorylated at a total of seven different phosphorylation sites (Table II). Two of the phosphorylation sites of the identified receptor-like kinases are novel sites, which have not been described previously (30). In addition, seven phosphorylation sites to five non-membrane protein kinases were identified. Among the receptor kinases, At5g10020 from the LRR III subfamily and At1g53730 and At3g14350 from the LRR V subfamily (54) showed a significant increase in relative phosphorylation after only 3 min at sites in the juxtamembrane region followed by a strong decrease already at 5 min of sucrose exposure. In contrast, a phosphopeptide from the C-terminal region of LRR III receptor kinase At3g02880 decreased significantly in relative phosphorylation after 30 min of sucrose resupply (Fig. 4*B*). Phosphopeptide ApSAEVLGK was conserved to the kinase domain of 10 different protein kinases (At3g02880, At5g53320, At5g16590, At4g23740, At3g08680, At5g05160, At3g17840, At5g58300, At1g48480, and At2g26730) and has also been identified previously (27).

One soluble protein kinase showed an increase in phosphorylation at a phosphorylation site in the kinase domain (peptide SYSTNLAFTPPEYLR; Fig. 4*B*) after 3 min of sucrose resupply but showed dephosphorylation at the N-terminal Thr-25 (peptide SNPDVTGLDEEGR; Fig. 4*B*) after 5 min. A very similar phosphopeptide identified from the kinase domain of a receptor-like cytoplasmic kinase II showed a more moderate response to sucrose treatment (peptide SYSTNLAYTPPEYLR; Fig. 4*B*). The protein kinase At4g35600 from the receptor-like cytoplasmic kinase IV family was phosphorylated in the kinase domain at Ser-117 after 5 min of sucrose resupply, and phosphorylation of the kinase At3g01490 increased after 10 min at a site located in the N-terminal region (Fig. 4*B*).

The two closely related phosphopeptides SYSTNLAFTPPEYLR and SYSTNLAYTPPEYLR of protein kinases At5g41260 and At4g35230, respectively, were clearly identified as different sequences based on their MS/MS fragmentation pattern (Fig. 5). Both peptides displayed a neutral loss

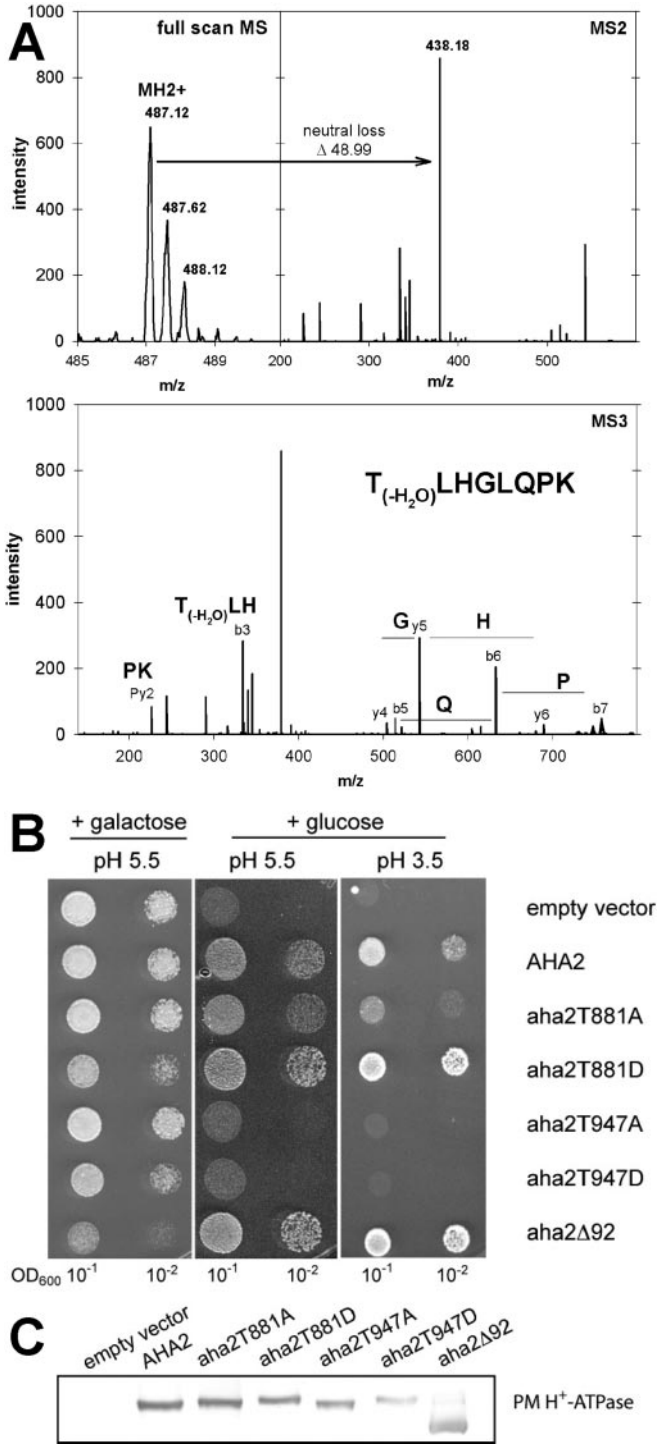

FIG. 3. **Identification of pTLHGLQPK and demonstration of its *in vivo* function.** *A*, full scan spectrum of doubly charged pTLHGLQPK, fragment spectrum with neutral loss, and subsequent MS/MS/MS fragmentation for sequence identification. *B*, yeast strains expressing mutated versions of AHA2 on galactose and glucose medium. On glucose medium growth of the yeast cells is dependent upon the activity of the plant H^+-ATPase. *C*, immunoblot demonstrating expression of plant plasma membrane (*PM*) H^+-ATPase in membranes of the transformed yeast lines used in this study (20 μg of yeast plasma membrane protein).

of 98, indicating serine or threonine phosphorylation. However, the information of the fragmentation pattern did not allow differentiation between phosphorylation of the first or the second serine in each of the peptides.

Other Proteins—A membrane protein with six transmembrane spans (At3g48740; related to nodulin MtN3 protein) was rapidly phosphorylated at Ser-247 located in the C terminus of the protein (Table II). The time course of relative phosphorylation for this membrane protein is very similar to that of the three receptor kinases with rapid increases in relative phosphorylation. Interestingly the protein displaying the most intense rapid decrease in phosphorylation was the peptide LpSFVR of a protein belonging to the remorin family. These are membrane-associated proteins with a hypothesized function in protein-protein interactions (55).

Specificity of the Response to Sucrose—To define sucrose specificity of the response, we carried out an experiment in which mannitol was resupplied to the sucrose-depleted seedlings. Interestingly the plasma membrane ATPase AHA2 showed no change in phosphorylation at the C-terminal peptide GLDIETPSHYpTV (Table II), whereas proton ATPase AHA1 did show increased phosphorylation of the C-terminal peptide GLDIDTAGHHYpTV (Table II). This indicates that there may indeed be specificity among the responses, and Thr-947 of AHA2 may more specifically be activated by sucrose. The phosphorylation site pSQLHELHA of aquaporin PIP2e (Table II) also showed an increase in relative phosphorylation after 5 min of resupply, indicating that this protein displays a general response to changes in osmotic conditions. The phosphorylation sites of the sucrose transporter and the three fast responding receptor kinases were not identified in the mannitol treatment.

DISCUSSION

This study is the first analysis of phosphorylation sites in plants that resolves a time course after a stimulus; in this case it was sucrose resupply after depletion. The regulation of sucrose sensing and uptake as well as regulation of sucrose metabolism is of utmost interest in plant biology. The possible sensing mechanisms involved have been under strong debate in the past (17, 56–58). In this study, a proteomics approach was taken to identify proteins that are rapidly modified by phosphorylation in response to sucrose. We further show that one of these phosphorylation sites is a novel site that determines the general activity state of the plasma membrane H^+-ATPase, an important protein providing the proton motive force that drives sucrose transport (59).

Recently comparative phosphoprotein analysis has yielded large datasets of elicitor responses in cell cultures (60), but temporal analysis of phosphorylation sites at the level of single phosphorylated peptides has not yet been studied in detail in plants. A temporal phosphoproteomics analysis of pathogenesis-related responses has been attempted using enrichment of phosphoproteins and iTRAQ (isobaric tags for

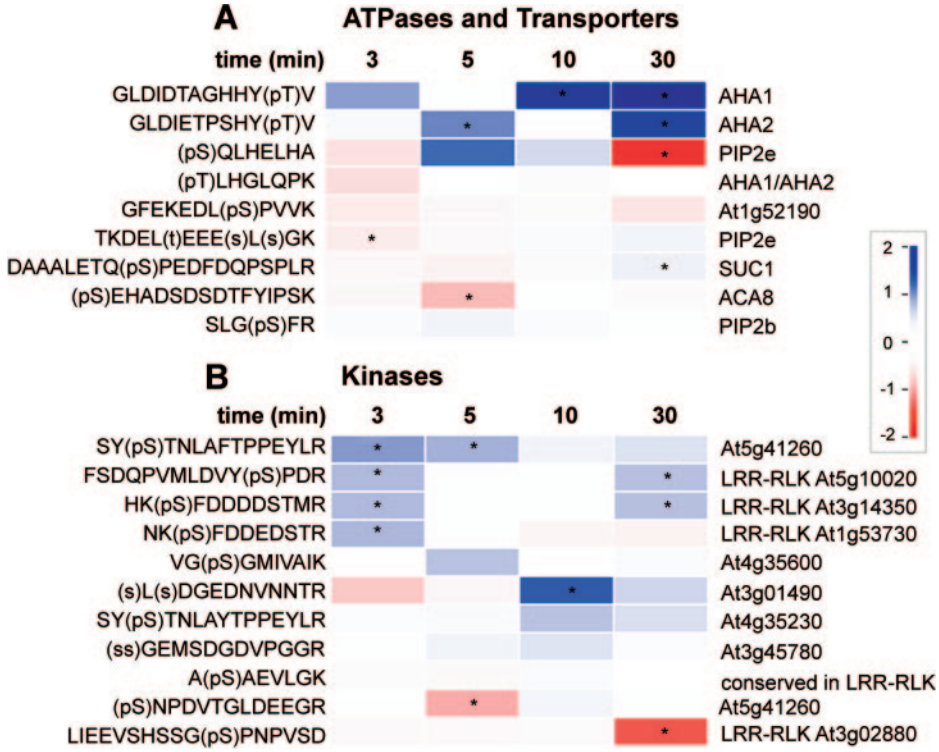

FIG. 4. **Changes in relative phosphorylation of different transport proteins and kinases in response to sucrose displayed as log_2-transformed ratios of normalized relative ion intensities at different time points.** *A*, responses of ATPases and transporters. *B*, responses of protein kinases. *Asterisks* indicate time points with significant increases or decreases as determined by pairwise least significant difference test ($p < 0.05$).

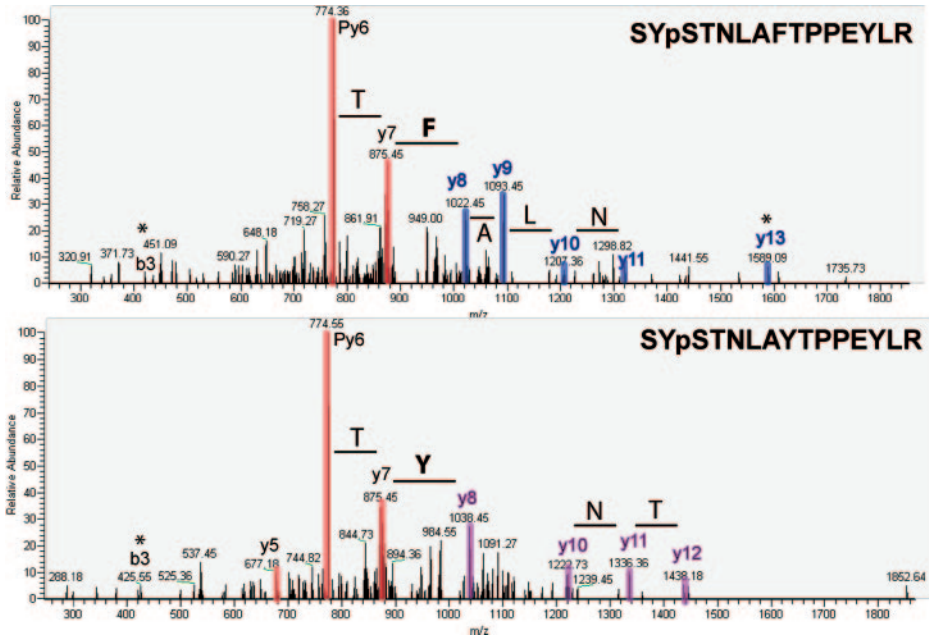

FIG. 5. **MS/MS fragmentation spectra for the phosphopeptides SYpSTNLAFTPPEYLR and SYpSTNLAYTPPEYLR of protein kinases At5g41260 and At4g35230, respectively.** The y ion series y8 to y12 indicates the differences between the two closely related sequences. Fragments indicative of phosphorylation are marked by *asterisks*.

relative and absolute quantification) labeling, but no phosphorylation sites were identified in that study (61). In mammalian systems an approach involving SILAC (stable isotope labeling by amino acids in cell culture) and subsequent immunoprecipitation of phosphorylated proteins has revealed ordered phosphorylation of proteins according to their position in a signaling cascade but was still lacking precise information of the actual phosphorylation sites involved (31). The first analysis of site-specific phosphorylation dynamics was carried out in yeast to analyze the response to mating pheromone (35) and has been optimized in mammalian cells, identifying site-specific phosphorylation dynamics (32).

With respect to phosphorylation site identification, in this study rather stringent criteria for the acceptance of phosphorylation sites were applied, and less starting material for plasma membrane preparation was used than in previous large scale studies. Although the number of identified sites in our study is 5 times lower than what has been published

previously for membrane preparations from cell cultures (27), 70% of the phosphorylation sites identified in this study are novel sites that had not been identified in previous work. The differences may be due to differences in tissue (cell culture *versus* seedlings) as well as to stress and condition-specific responses. However, there is no bias toward certain classes of proteins identified in our study *versus* previous work.

Because metabolic labeling of whole plant seedlings is a rather lengthy task over at least two plant generations, we chose a label-free approach for relative comparison of ion intensities between samples that was used successfully before to characterize the proteome of the human centrosome (62). The variation of retention times between the five different LC runs was around 1%, which still allowed efficient peak assignment based on *m/z* values and their retention times between different samples. The average relative error of quantitation per protein as calculated from the mean ratios of analytical replicates ranged from 6 to 20%, which is slightly higher than what has been noted for metabolic stable isotope labeling approaches (63). We were able to (i) reproduce the response of the most common peptides in independent biological experiments (Supplemental Fig. 2) and (ii) validate the result of the label-free quantitation in the case of the plasma membrane ATPase in which the relationship between C-terminal phosphorylation and protein activity is well described (59). By label-free quantitation we found an increase in phosphorylation of C-terminal peptides GLDIETPSHYpTV and GLDIDTAGHHYpTV, and this clearly was accompanied by an increase in proton pumping activities in sucrose-supplied plasma membrane vesicles. Thus, the quantitation method indeed yields information relevant for the biology of the system under investigation.

In this study, we clearly identified 67 phosphorylation sites. Among the identified phosphorylation sites, we also confirmed well known sites, such as the C-terminal threonine of plasma membrane ATPases or known regulatory sites of aquaporins. In those cases, the time course of the relative intensities of the respective phosphopeptides is in good agreement with known biochemical and structural properties of these proteins or their activation or inactivation status. In addition, we clearly established an *in vivo* relevance for one of the new phosphorylation sites of AHA2 in controlling activity of the proton ATPase. Therefore, we are convinced that temporal analysis of phosphorylation sites using a label-free protein correlation approach is a suitable strategy to gain valuable insights into the regulatory processes involved in the specific response under investigation in tissues and systems not suited for metabolic labeling. Moreover the conserved phosphorylation site Ser-278 in the C terminus of PIP2e was found to have increased phosphorylation, suggesting that addition of sucrose leads to activation potentially via a transregulation within the complex as recently found for the ammonium transporter AMT1;1 (53). The novel sucrose transporter phosphorylation site may play an important role in acclimating sucrose uptake to the extracellular supply. Further work using site-directed mutagenesis is required to determine the role of this site in regulation of sucrose transport.

The *Arabidopsis* proteome is far from being annotated completely, and a large fraction of proteins still have no function assigned. In that respect, studies of the dynamic behavior and the analysis of phosphorylation under different conditions may provide a valuable contribution to the functional categorization of yet poorly annotated proteins. For example, two "unknown" proteins (At1g15400 and At5g57110; Table II) were identified in this study that showed temporal behavior of phosphorylation similar to that of the plasma membrane Ca^{2+}-transporting ATPase ACA8. Similarly the uncharacterized protein kinase At5g41260 (Fig. 4*B*) could be involved in sucrose-related or osmotic responses.

Especially the changes in relative phosphorylation of kinases may reveal interesting information about signaling pathways. For example, in this study three membrane-bound kinases were identified that showed a rapid transient change in relative phosphorylation, whereas the identified soluble kinases showed peaks in relative phosphorylation at later time points. It certainly is too early to draw a direct connection or a signaling cascade, but further and more detailed similar phosphorylation dynamics studies under different nutrient conditions may help to identify such connections. In combination with bioinformatics analysis tools about domain structure (*e.g.* SMART (Simple Modular Architecture Research Tool), European Molecular Biology Laboratory) or short, characteristic sequence motifs (*e.g.* ELM (Eukaryotic Linear Motif), the ELM Consortium) and with thorough clustering analysis of the identified responses we may gain more insight into the links between patterns of phosphorylation and possible function of unknown proteins. Clustering of the quantified phosphorylation sites identified in this study revealed four significant response classes (Fig. 6). Interestingly the protein distribution between these classes shows that the kinases identified in our study exclusively group in clusters 1 and 2, which on average show rapid increases or decreases of relative phosphorylation. In contrast, enzymes and other proteins are more represented in "slow" responding clusters 3 and 4. Clustering of the responses may therefore be an important tool to identify proteins involved in a signaling cascade in a time-resolved manner especially if this type of analysis is being extended over a wide range of conditions in a large scale fashion. Of course, detailed functional characterizations of candidate proteins will ultimately have to go hand in hand with the analysis of the respective T-DNA insertional mutants and will have to include transcriptomics and metabolomics profiling.

Recently a detailed analysis of the temporal transcriptional responses was carried out in seedlings under sucrose depletion and resupply in combination with whole plant analysis under conditions of endogenous sucrose limitation (10). In these experiments, transcript levels of the sucrose transporter

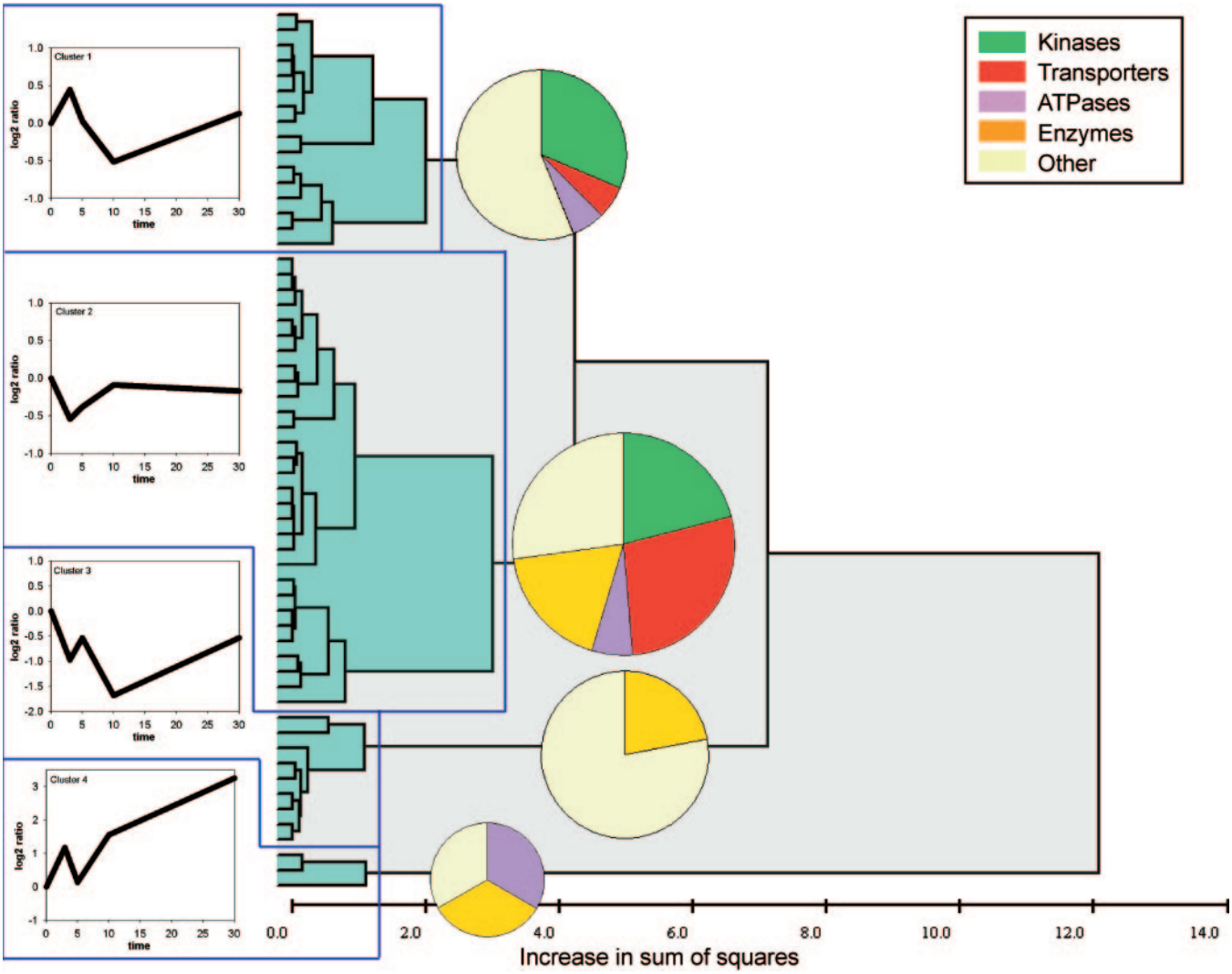

FIG. 6. **Clustering of time responses of the quantified phosphorylation sites by increase in sum of squares (Ward's method) reveals four significant response clusters as determined by greatest deviation from clusters in randomized datasets.** *Graphs* show the mean response curve of all members of that cluster. *Pie charts* display the functional classification of proteins in a given response cluster. The fraction of kinases is higher in the two classes with rapid increase or decreasing responses.

SUC1 increased after 3 h of sucrose resupply, whereas transcript levels of the proton ATPase AHA1 or aquaporin PIP2e remained unchanged under those conditions. More interestingly two of the receptor kinases (At1g53730 and At3g14350) identified here with sucrose-responsive phosphorylation patterns are up-regulated transcriptionally in plants under endogenous sucrose depletion (starchless *pgm* mutant). These findings indicate that protein phosphorylation provides another layer of regulation that may not affect transcription, whereas in some cases specific proteins/genes may be affected on both regulatory levels. Our work contributes to and sets the stage for these yet unrecognized regulatory patterns especially with respect to very short term changes in environmental conditions for the plant.

With this work we have made a first step in including a dynamic component to plant phosphoproteomics. Although in total the fraction of phosphorylation sites for which quantitative time course information could be resolved was rather low (65% of all identified sites), we believe that with more optimization of phosphopeptide enrichment, larger quantities of starting material, and alternative MS/MS fragmentation techniques the number can well be exceeded. Nevertheless the results presented in this first study of dynamic plant phosphoproteomics already indicate exciting new candidates possibly involved in the key process of sucrose transport and regulation. These will be validated in in-depth biological experiments in the future. However, it is important to point out that this unbiased proteomics survey study provided a terrific basis for novel targeted analyses in a field that has been under intense investigation for a long time in plant biology.

In conclusion, our work on dynamics of phosphorylation under sucrose depletion and resupply validates the method of

protein correlation profiling as an alternative approach for quantitation in cases where metabolic labeling is not possible (*i.e.* tissue samples, whole plant, and seedlings). Furthermore we clearly identified several previously undescribed phosphorylation sites even in well studied proteins such as the plasma membrane proton ATPases, and most importantly, we give first insights into the dynamic behavior of individual phosphorylation sites under specific conditions. We believe that similar experiments carried out under different stress conditions will provide a strong basis for our understanding of signaling processes in plants.

Acknowledgments—We thank Pawel Durek and Dr. Dirk Walther for help with Java scripts and clustering analysis and Anette Lund for technical assistance.

* This work has been supported by the Human Frontier Science Program Fellowship (to T. N.), Danish Research Council for Technology and Production Grant FTP-274-05-0269 (to M. G. P.), and Department of Energy Grant DE-FG02-04ER15542 (to W. B. F.). The costs of publication of this article were defrayed in part by the payment of page charges. This article must therefore be hereby marked "*advertisement*" in accordance with 18 U.S.C. Section 1734 solely to indicate this fact.

S The on-line version of this article (available at http://www.mcponline.org) contains supplemental material.

§ Both authors made equal contributions to this work.

** Supported by the Emmy-Noether Program of the Deutsche Forschungsgemeinschaft. To whom correspondence should be addressed. E-mail: wschulze@mpimp-golm.mpg.de.

REFERENCES

1. Chiou, T. J., and Bush, D. R. (1998) Sucrose is a signal molecule in assimilate partitioning. *Proc. Natl. Acad. Sci. U. S. A.* **95,** 4784–4788
2. Huber, S. C., and Huber, J. L. (1996) Role and regulation of sucrose-phosphate-synthase in higher plants. *Annu. Rev. Plant Physiol. Plant Mol. Biol.* **47,** 431–444
3. Loewe, A., Einig, W., and Hampp, R. (1996) Coarse and fine control and annual changes of sucrose-phosphate synthase in Norway spruce needles. *Plant Physiol.* **112,** 641–649
4. Winter, H., and Huber, S. C. (2000) Regulation of sucrose metabolism in higher plants: localization and regulation of activity of key enzymes. *Crit. Rev. Biochem. Mol. Biol.* **35,** 253–289
5. Kim, J. H., and Johnston, M. (2006) Two glucose-sensing pathways converge on Rgt1 to regulate expression of glucose transporter genes in Saccharomyces cerevisiae. *J. Biol. Chem.* **281,** 26144–26149
6. Quick, W., Schurr, U., Scheibe, R., Schulze, E. D., Rodermel, S. R., Bogorad, L., and Stitt, M. (1991) Decreased ribulose-1,5-bisphosphate carboxylase-oxygenase in transgenic tobacco transformed with "antisense" *rbcS*. I. Impact on photosynthesis in ambient growth conditions. *Planta* **183,** 542–554
7. Nielsen, T. H., Krapp, A., Roper-Schwarz, U., and Stitt, M. (1998) The sugar-mediated regulation of genes encoding the small subunit of Rubisco and the regulatory subunit of ADP glucose pyrophosphorylase is modified by phosphate and nitrogen. *Plant Cell Environ.* **21,** 443–454
8. Bernier, G., Havelange, A., Houssa, C., Petitjean, A., and Lejeune, P. (1993) Physiological signals that induce flowering. *Plant Cell* **5,** 1147–1155
9. Sonnewald, U., Hajirezaei, M. R., Kossmann, J., Heyer, A., Trethewey, R. N., and Willmitzer, L. (1997) Increased potato tuber size resulting from apoplastic expression of a yeast invertase. *Nat. Biotechnol.* **15,** 794–797
10. Osuna, D., Usadel, B., Morcuende, R., Gibon, Y., Bläsing, O. E., Höhne, M., Günter, M., Kamlage, B., Trethewey, R., Scheible, W. R., and Stitt, M. (2007) Temporal responses of transcripts, enzyme activities and metabolites after adding sucrose to carbon-deprived Arabidopsis seedlings. *Plant J.* **49,** 463–491
11. Smeekens, S. C. M. (2000) Sugar-induced signal transduction in plants. *Annu. Rev. Plant Physiol. Plant Mol. Biol.* **51,** 49–81
12. Rook, F., Gerrits, N., Kortsett, A., van Kampe, M., and Borrias, M. (1998) Sucrose specific signalling represses translation of the Arabidopsis *ATB2* bZIP transcription factor gene. *Plant J.* **15,** 256–263
13. Vaughn, M. W., Harrington, G. N., and Bush, D. R. (2002) Sucrose-mediated transcriptional regulation of sucrose symporter activity in the phloem. *Proc. Natl. Acad. Sci. U. S. A.* **99,** 10876–10880
14. Ransom-Hodgkins, W. D., Vaughn, M. W., and Bush, D. R. (2003) Protein phosphorylation plays a key role in sucrose-mediated transcriptional regulation of a phloem-specific proton-sucrose symporter. *Planta* **217,** 483–489
15. Moore, B., Zhou, L., Rolland, F., Hall, Q., Cheng, W.-H., Liu, Y.-X., Hwang, I., Jones, T., and Sheen, J. (2003) Role of the Arabidopsis glucose sensor HXK1 in nutrient, light and hormonal signaling. *Science* **300,** 332–336
16. Cho, Y. H., Yoo, S. D., and Sheen, J. (2006) Regulatory functions of nuclear hexokinase1 complex in glucose signaling. *Cell* **127,** 579–589
17. Barker, L., Kühn, C., Weise, A., Schulz, A., Gebhardt, C., Hirner, B., Hellmann, H., Schulze, W., Ward, J. M., and Frommer, W. B. (2000) SUT2, a putative sucrose sensor in sieve elements. *Plant Cell* **12,** 1153–1164
18. Reinders, A., Schulze, W., Thaminy, S., Stagljar, I., Frommer, W. B., and Ward, J. M. (2002) Intra- and intermolecular interactions in sucrose transporters at the plasma membrane detected by the split-ubiquitin system and functional assays. *Structure* (*Lond.*) **10,** 763–772
19. Chung, H. J., Sehnke, P. C., and Ferl, R. J. (1999) The 14-3-3 proteins: cellular regulators of plant metabolism. *Trends Plant Sci.* **4,** 367–371
20. Yaffe, M. B. (2002) Phosphotyrosine-binding domains in signal transduction. *Nat. Rev. Mol. Cell. Biol.* **3,** 177–186
21. Pawson, T. (2004) Specificity in signal transduction: from phosphotyrosine-SH2 domain interactions to complex cellular systems. *Cell* **116,** 191–203
22. Pawson, T., and Gish, G. D. (1992) SH2 and SH3 domains: from structure to function. *Cell* **71,** 359–362
23. Camoni, L., Iori, V., Marra, M., and Aducci, P. (2000) Phosphorylation-dependent interaction between plant plasma membrane H^+-ATPase and 14-3-3 proteins. *J. Biol. Chem.* **275,** 99919–99923
24. Hrabak, E. M., Chan, C. W., Gribskov, M., Harper, J. F., Choi, J. H., Halford, N., Kudla, J., Luan, S., Nimmo, H. G., Sussman, M. R., Thomas, M., Walker-Simmons, K., Zhu, J. K., and Harmon, A. C. (2003) The Arabidopsis CDPK-SnRK superfamily of protein kinases. *Plant Physiol.* **132,** 666–680
25. Wang, X., Goshe, M. B., Sonderblom, E. J., Phinney, B. S., Kuchar, J. A., Li, J., Asami, T., Yoshida, S., Huber, S. C., and Clouse, S. D. (2005) Identification and functional analysis of in vivo phosphorylation sites of the Arabidopsis Brassinosteroid-insensitive 1 receptor kinase. *Plant Cell* **17,** 1685–1703
26. Yoshida, S., and Parniske, M. (2005) Regulation of plant symbiosis receptor kinase through serine and threonine phosphorylation. *J. Biol. Chem.* **280,** 9203–9209
27. Nühse, T. S., Stensballe, A., Jensen, O. N., and Peck, S. C. (2004) Phosphoproteomics of the Arabidopsis plasma membrane and a new phosphorylation site database. *Plant Cell* **16,** 2394–23405
28. Hegeman, A. D., Harms, A. C., Sussman, M. R., Bunner, A. E., and Harper, J. F. (2004) An isotope labeling strategy for quantifying the degree of phosphorylation at multiple sites in proteins. *J. Am. Soc. Mass Spectrom.* **15,** 647–653
29. Wolschin, F., and Weckwerth, W. (2005) Combining metal oxide affinity chromatography (MOAC) and selective mass spectrometry for robust identification of in vivo protein phosphorylation sites. *Plant Methods* **1,** 1–10
30. Nühse, T. S., Stensballe, A., Jensen, O. N., and Peck, J. (2003) Large-scale analysis of *in vivo* phosphorylated membrane proteins by immobilized metal ion affinity chromatography and mass spectrometry. *Mol. Cell. Proteomics* **2,** 1234–1243
31. Blagoev, B., Ong, S.-E., Kratchmarova, I., and Mann, M. (2004) Temporal ordering of signaling networks by quantitative proteomics. *Nat. Biotechnol.* **22,** 1139–1145
32. Olsen, J. V., Blagoev, B., Gnad, F., Macek, B., Kumar, C., Mortensen, P., and Mann, M. (2006) Global, in vivo, and site-specific phosphorylation dynamics in signaling networks. *Cell* **127,** 635–648
33. Axelsen, K. B., Venema, K., Jahn, T., Baunsgaard, L., and Palmgren, M. G. (1999) Molecular dissection of the C-terminal regulatory domain of the plant plasma membrane H^+-ATPase AHA2: mapping of residues that

when altered give rise to an activated enzyme. *Biochemistry* **38,** 7227–7234
34. Rappsilber, J., Ishihama, Y., and Mann, M. (2003) Stop and go extraction tips for matrix-assisted laser desorption/ionization, nanoelectrospray, and LC/MS sample pretreatment in proteomics. *Anal. Chem.* **75,** 663–670
35. Gruhler, A., Olsen, J. V., Mohammed, S., Mortensen, P., Faergman, N., Mann, M., and Jensen, O. N. (2005) Quantitative phosphoproteomics applied to the yeast pheromone signaling pathway. *Mol. Cell. Proteomics* **4,** 310–327
36. Elias, J. E., and Gygi, S. P. (2007) Target-decoy search strategy for increased confidence in large-scale protein identifications by mass spectrometry. *Nat. Methods* **4,** 207–214
37. Andersen, J. R., Lyon, C. E., Fox, A. H., Leung, A. K. L., Lam, Y. W., Steen, H., Mann, M., and Lamond, A. I. (2002) Direct proteomic analysis of the human nucleolus. *Curr. Biol.* **12,** 1–11
38. Steen, H., Jebanathirajah, J. A., Springer, M., and Kirschner, M. W. (2005) Stable isotope-free relative and absolute quantitation of protein phosphorylation stoichiometry by MS. *Proc. Natl. Acad. Sci. U. S. A.* **102,** 3948–3953
39. Fuglsang, A. T., Borch, J., Bych, K., Jahn, T. P., Roepstorff, P., and Palmgren, M. G. (2003) The binding site for regulatory 14-3-3 protein in plant plasma membrane H^+-ATPase: involvement of a region promoting phosphorylation-independent interaction in addition to the phosphorylation-dependent C-terminal end. *J. Biol. Chem.* **278,** 42266–42272
40. Buch-Pedersen, M. J., Venema, K., Serrano, R., and Palmgren, M. G. (2000) Abolishment of proton pumping and accumulation in the E1P conformational state of a plant plasma membrane H^+-ATPase by substitution of a conserved aspartyl residue in transmembrane segment 6. *J. Biol. Chem.* **275,** 39167–39173
41. Fuglsang, A. T., Visconti, S., Drumm, K., Jahn, T., Stensballe, A., Mattei, B., Jensen, O. N., Aducci, P., and Palmgren, M. G. (1999) Binding of 14-3-3 protein to the plasma membrane H^+-ATPase AHA2 involves the three C-terminal residues Tyr^{946}-Thr-Val and requires phosphorylation of Thr^{947}. *J. Biol. Chem.* **274,** 36774–36780
42. Palmgren, M. G., Sommarin, M., Serrano, R., and Larsson, C. (1991) Identification of an autoinhibitory domain in the C-terminal region of the plant plasma membrane H^+-ATPase. *J. Biol. Chem.* **266,** 20470–20475
43. Nelson, C. J., Hegeman, A. D., Harms, A. C., and Sussman, M. R. (2006) A quantitative analysis of Arabidopsis plasma membrane using trypsin-catalyzed ^{18}O labeling. *Mol. Cell. Proteomics* **5,** 1382–1395
44. Olsson, A., Svennelid, F., Ek, B., Sommarin, M., and Larsson, C. (1998) A phosphothreonine residue at the C-terminal end of the plasma membrane H^+-ATPase is protected by fusicoccin-induced 14-3-3 binding. *Plant Physiol.* **118,** 551–555
45. Svennelid, F., Olsson, A., Piotrowski, M., Rosenquist, M., Ottman, C., Larsson, C., Öcking, C., and Sommarin, M. (1999) Phosphorylation of Thr-948 at the C terminus of the plasma membrane H^+-ATPase creates a binding site for the regulatory 14-3-3 protein. *Plant Cell* **11,** 2379–2391
46. Würtele, M., Jelich-Ottmann, C., Wittinghofer, A., and Öcking, C. (2003) Structural view of a fungal toxin acting on a 14-3-3 regulatory complex. *EMBO J.* **22,** 987–994
47. Sze, H., Liang, F., Hwang, I., Curran, A. C., and Harper, J. F. (2000) Diversity and regulation of plant Ca^{2+} pumps: insights from expression in yeast. *Annu. Rev. Plant Physiol. Plant Mol. Biol.* **51,** 433–462
48. Huang, J. Z., Hardin, S. C., and Huber, S. C. (2001) Identification of a novel phosphorylation motif for CDPKs: phosphorylation of synthetic peptides lacking basic residues at P-3/P-4. *Arch. Biochem. Biophys.* **393,** 61–66
49. Roblin, G., Sakr, S., Bonmort, J., and Delrot, S. (1998) Regulation of a plant plasma membrane sucrose transporter by phosphorylation. *FEBS Lett.* **424,** 165–168
50. Schulze, W., Weise, A., Frommer, W. B., and Ward, J. M. (2000) Function of the cytosolic N-terminus of sucrose transporter AtSUT2 in substrate affinity. *FEBS Lett.* **485,** 189–194
51. Kühn, C., Franceschi, V. R., Schulz, A., Lemoine, R., and Frommer, W. B. (1997) Macromolecular trafficking indicated by localization and turnover of sucrose transporters in enucleate sieve elements. *Science* **275,** 1298–1300
52. Tornroth-Horsefield, S., Wang, Y., Hedfalk, K., Johanson, U., Karlsson, M., Tajkhorshid, E., Neutze, R., and Kjellbom, P. (2006) Structural mechanism of plant aquaporin gating. *Nature* **439,** 688–694
53. Loque, D., Lalonde, S., Looger, L. L., von Wiren, N., and Frommer, W. B. (2007) A cytosolic trans-activation domain essential for ammonium uptake. *Nature* **446,** 195–198
54. Shiu, S.-H., and Bleecker, A. B. (2001) Plant receptor-like kinase gene family: diversity, function, and signaling. *Sci. STKE* **113,** 1–13
55. Bariola, P. A., Retelska, D., Stasiak, A., Kammerer, R. A., Fleming, A., Hijri, M., Frank, S., and Farmer, E. E. (2004) Remorins form a novel family of coiled coil-forming oligomeric and filamentous proteins associated with apical, vascular and embryonic tissues in plants. *Plant Mol. Biol.* **55,** 579–594
56. Schulze, W., Reinders, A., Ward, J. M., Lalonde, S., and Frommer, W. B. (2003) Interactions between co-expressed Arabidopsis sucrose transporters in the split-ubiquitin system. *BMC Biochem.* **4,** 3
57. Barth, I., Meyer, S., and Sauer, N. (2003) PmSUC3: characterization of a SUT2/SUC3-type sucrose transporter from *Plantago major*. *Plant Cell* **15,** 1375–1385
58. Eckardt, N. A. (2003) The function of SUT2/SUC3 sucrose transporters: the debate continues. *Plant Cell* **14,** 1259–1262
59. Palmgren, M. G. (2001) Plant plasma membrane H^+-ATPases: powerhouses for nutrient uptake. *Annu. Rev. Plant Physiol. Plant Mol. Biol.* **52,** 817–845
60. Benschop, J. J., Mohammed, S., O'Flaherty, M., Heck, A. J., Slijper, M., and Menke, F. L. (2007) Quantitative phosphoproteomics of early elicitor signaling in Arabidopsis. *Mol. Cell. Proteomics* **6,** 1198–1214
61. Jones, A. M., Bennett, M. H., Mansfield, J. W., and Grant, M. (2006) Analysis of the defence phosphoproteome of Arabidopsis thaliana using differential mass tagging. *Proteomics* **6,** 4155–4165
62. Andersen, J. S., Wilkinson, C. J., Myoru, T., Mortensen, P., Nigg, E. A., and Mann, M. (2003) Proteomic characterization of the human centrosome by protein correlation profiling. *Nature* **426,** 570–574
63. Ong, S.-E., Kratchmarova, I., and Mann, M. (2003) Properties of ^{13}C-substituted arginine in stable isotope labeling by amino acids in cell culture (SILAC). *J. Proteome Res.* **2,** 173–181